

## ARTICLE

**Structural and Infrared Spectroscopic Study on Solvation of Acetylene by Protonated Water Molecules<sup>†</sup>**

Xiang-tao Kong<sup>a</sup>, Xin Lei<sup>a</sup>, Qin-qin Yuan<sup>a</sup>, Bing-bing Zhang<sup>a,b</sup>, Zhi Zhao<sup>a,c</sup>, Dong Yang<sup>a</sup>,  
Shu-kang Jiang<sup>a</sup>, Dong-xu Dai<sup>a</sup>, Ling Jiang<sup>a\*</sup>

*a.* State Key Laboratory of Molecular Reaction Dynamics, Collaborative Innovation Center of Chemistry for Energy and Materials, Dalian Institute of Chemical Physics, Chinese Academy of Sciences, Dalian 116023, China

*b.* State Key Laboratory of Fine Chemicals, Dalian University of Technology, Dalian 116024, China

*c.* Key Laboratory of Materials Modification by Laser, Ion and Electron Beams, Dalian University of Technology, Ministry of Education, Dalian 116024, China

(Dated: Received on November 19, 2015; Accepted on December 11, 2015)

The effect of solvation on the conformation of acetylene has been studied by adding one water molecule at a time. Quantum chemical calculations of the  $\text{H}^+(\text{C}_2\text{H}_2)(\text{H}_2\text{O})_n$  ( $n=1-5$ ) clusters indicate that the  $\text{H}_2\text{O}$  molecules prefer to form the  $\text{OH}\cdots\pi$  interaction rather than the  $\text{CH}\cdots\text{O}$  interaction. This solvation motif is different from that of neutral  $(\text{C}_2\text{H}_2)(\text{H}_2\text{O})_n$  ( $n=1-4$ ) clusters, in which the  $\text{H}_2\text{O}$  molecules prefer to form the  $\text{CH}\cdots\text{O}$  and  $\text{OH}\cdots\text{C}$  H-bonds. For the  $\text{H}^+(\text{C}_2\text{H}_2)(\text{H}_2\text{O})_n$  cationic clusters, the first solvation shell consists of one ring structure with two  $\text{OH}\cdots\pi$  H-bonds and three water molecules, which is completed at  $n=4$ . Simulated infrared spectra reveal that vibrational frequencies of  $\text{OH}\cdots\pi$  H-bonded O–H stretching afford a sensitive probe for exploring the solvation of acetylene by protonated water molecules. Infrared spectra of the  $\text{H}^+(\text{C}_2\text{H}_2)(\text{H}_2\text{O})_n$  ( $n=1-5$ ) clusters could be readily measured by the infrared photodissociation technique and thus provide useful information for the understanding of solvation processes.

**Key words:** Acetylene, Water, Solvation, Infrared photodissociation spectroscopy, Quantum chemical calculation

**I. INTRODUCTION**

Hydrogen-bonded interactions are of considerable interest because of their significant importance in physical, chemical, atmospheric, biological sciences, and so on [1–7]. The classical hydrogen bonds (H-bonds) are usually defined as  $\text{A}-\text{H}\cdots\text{B}$  interactions, where  $\text{A}-\text{H}$  is a proton donating bond and  $\text{B}$  is a proton accepting center that has at least one lone electron pair.  $\text{A}$  and  $\text{B}$  are electronegative atoms, such as  $\text{O}$ ,  $\text{N}$ ,  $\text{F}$ , and  $\text{Cl}$ . Extensive efforts have also been made to study new types of H-bonds, which include nonconventional proton donors (*i.e.*,  $\text{C}-\text{H}$ ) and proton acceptors (*i.e.*,  $\pi$ -bonded functional groups), as well as dihydrogen bonds [8–13].

Fully rotationally resolved spectra have demonstrated that water is positioned above the benzene plane, forming the  $\text{OH}\cdots\pi$  H-bonded interactions [14]. Resonant ion-dip infrared spectroscopy of the  $\text{C}_6\text{H}_6(\text{H}_2\text{O})_n$  ( $n=1-7$ ) clusters has indicated that there

exist both classical  $\text{OH}\cdots\text{O}$  and nonconventional  $\text{OH}\cdots\pi$  H-bonded interactions [15]. The  $\text{NH}\cdots\pi$  H-bonded interactions have been detected in the ammonia-benzene dimer by high-resolution optical and microwave spectra [16]. High-level *ab initio* calculations have exhibited that the  $\text{OH}\cdots\pi$  H-bond in  $\text{C}_6\text{H}_6-\text{H}_2\text{O}$  is stronger than the  $\text{NH}\cdots\pi$  H-bond in  $\text{C}_6\text{H}_6-\text{NH}_3$ , and their directionality is mainly controlled by the electrostatic interaction [17]. The  $\text{CH}\cdots\pi$  H-bonded energy in  $\text{C}_6\text{H}_6-\text{CH}_4$  is determined to be 4.31–4.73 kJ/mol by mass analyzed threshold ionization spectroscopy, which is consistent with the theoretical value calculated by the CCSD(T) method [18]. In the interactions of ethylene with the first-row hydrides ( $\text{CH}_4$ ,  $\text{NH}_3$ ,  $\text{H}_2\text{O}$ , and  $\text{HF}$ ),  $\pi$  H-bonds become stronger from  $\text{CH}_4$  to  $\text{HF}$ , which is highly correlated to inductive energy [19].

The  $\text{OH}\cdots\pi$  H-bond could also be formed in the interactions of water with the simplest alkyne, acetylene. Previous studies have revealed that  $(\text{C}_2\text{H}_2)(\text{H}_2\text{O})$  has two configurations, in which either  $\text{H}_2\text{O}$  acts as proton acceptor to form  $\text{CH}\cdots\text{O}$  H-bond or  $\text{C}_2\text{H}_2$  serves as proton acceptor to form  $\text{OH}\cdots\pi$  H-bond. The  $\text{CH}\cdots\text{O}$  H-bond is stronger than the  $\text{OH}\cdots\pi$  H-bond, and the barrier for the isomerization from the latter to the former is very low (0.75 kJ/mol), suggesting that the interconversion readily occurs [11, 20]. Theoretical inves-

<sup>†</sup>Part of the special issue for “the Chinese Chemical Society’s 14th National Chemical Dynamics Symposium”.

\*Author to whom correspondence should be addressed. E-mail: ljjiang@dicp.ac.cn.

tigations of neutral  $(\text{C}_2\text{H}_2)(\text{H}_2\text{O})_n$  ( $n=1-4$ ) clusters have indicated that the interactions between acetylene and water are mainly composed by  $\text{CH}\cdots\text{O}$  and  $\text{OH}\cdots\text{C}$  H-bonds [21, 22]. When acetylene interacts with protonated water molecule ( $\text{H}_3\text{O}^+$ ), only one stable configuration with  $\text{OH}\cdots\pi$  H-bond is formed, which binding energy was predicted to be 81.13 kJ/mol at MP2/6-311++G(3df,3pd) level [5]. So far, much less work has been done for the systematic study on the solvation of  $\text{C}_2\text{H}_2$  by protonated water clusters, leaving that the issues how the excess proton affects solvation motif of  $\text{C}_2\text{H}_2$  as compared to the neutral water and how the  $\text{OH}\cdots\pi$  H-bond varies with sequential hydration remain open.

Herein, we present a study on the solvation of  $\text{C}_2\text{H}_2$  by a series of protonated water clusters. Electronic structure calculations of the  $\text{H}^+(\text{C}_2\text{H}_2)(\text{H}_2\text{O})_n$  ( $n=1-5$ ) clusters reveal that the  $\text{H}_2\text{O}$  molecules prefer to form the  $\text{OH}\cdots\pi$  interaction rather than the  $\text{CH}\cdots\text{O}$  interaction. The first solvation shell consists of one ring structure with two  $\text{OH}\cdots\pi$  H-bonds and three water molecules, which is completed at  $n=4$ . Simulated IR spectra exhibit that vibrational frequencies of  $\text{OH}\cdots\pi$  H-bonded O–H stretching afford a sensitive probe for exploring the solvation of acetylene by adding one water molecule at a time.

## II. THEORETICAL METHODS

Quantum chemical calculations are carried out using Gaussian 09 program suite [23]. Initial configurations are built on the basis of the relevant structures reported in Refs.[5, 21, 22]. Previous investigations have demonstrated that the structures and energetics of H-bonded complexes could be properly predicted by the M06-2X hybrid functional [24–27], which functional is employed for the present calculations. The aug-cc-pVDZ basis set is used for C, H, and O atoms. Tight convergence of the optimization and the self-consistent field procedures is imposed, and an ultrafine grid is utilized. Relative energies include zero-point vibrational energies. Harmonic vibrational frequencies are calculated at the same level. All reported structures are true minima without imaginary vibrational frequencies. Simulated IR spectra are derived from M06-2X/aug-cc-pVDZ harmonic vibrational frequencies and intensities. Harmonic vibrational frequencies are scaled by a factor of 0.933, which is determined by the comparison of simulated vibrational frequencies of the bridged proton stretch in the nonclassical  $\text{H}^+(\text{C}_2\text{H}_2)$  ion with experimental value [28]. IR stick spectra are convoluted by a Gaussian line shape function with a width of  $10\text{ cm}^{-1}$ . The quantum theory of “atoms in molecules” calculations are performed by the Multiwfn program at the M06-2X/aug-cc-pVDZ level [29].

## III. RESULTS AND DISCUSSION

### A. Solvation motifs and IR spectra

Several representative low-lying structures of the  $\text{H}^+(\text{C}_2\text{H}_2)(\text{H}_2\text{O})_n$  ( $n=1-5$ ) clusters are presented in Fig.1. The structures are labeled according to the number of  $\text{H}_2\text{O}$  molecules and relative energies. For each cluster up to  $n=5$ , simulated IR spectra of the representative low-lying isomers are shown in Figs.2–5. Scaled harmonic vibrational frequencies and intensities of free O–H stretching,  $\text{OH}\cdots\pi$  H-bonded O–H stretching,  $\text{OH}\cdots\text{O}$  H-bonded O–H stretching, and C–H stretching of  $\text{C}_2\text{H}_2$  in the lowest-lying isomers of  $\text{H}^+(\text{C}_2\text{H}_2)(\text{H}_2\text{O})_n$  ( $n=1-5$ ) are listed in Table I.

#### 1. $n=1$

As illustrated in Fig.1, one OH group of the  $\text{H}_3\text{O}^+$  moiety in the isomer 1A forms one  $\text{OH}\cdots\pi$  H-bond with  $\pi$  electrons of  $\text{C}_2\text{H}_2$ , leaving other two OH groups free.

Four kinds of absorption peaks are mainly observed in 1A (Fig.2). The frequencies at  $3536$  and  $3449\text{ cm}^{-1}$  are assigned to the free O–H stretching vibration of  $\text{H}_3\text{O}^+$  (labeled free  $\nu_{\text{OH}}$ ) (Table I). The frequency at  $3134\text{ cm}^{-1}$  corresponds to the C–H stretching vibrations of  $\text{C}_2\text{H}_2$  (labeled  $\nu_{\text{CH}}$ ). Sharp peak at  $2036\text{ cm}^{-1}$  belongs to the  $\text{OH}\cdots\pi$  H-bonded O–H stretching (labeled  $\nu_{\text{OH}\cdots\pi}$ ). The  $\text{C}\equiv\text{C}$  stretching vibration (labeled  $\nu_{\text{C}\equiv\text{C}}$ ) is predicted at  $1920\text{ cm}^{-1}$ .

#### 2. $n=2$

On the basis of 1A, the second  $\text{H}_2\text{O}$  either binds to  $\text{H}_3\text{O}^+$  (isomer 2A) or one CH end of acetylene (isomer 2B). The isomer 2B consists of one  $\text{OH}\cdots\pi$  H-bond and one  $\text{CH}\cdots\text{O}$  H-bond, which lies  $64.03\text{ kJ/mol}$  above 2A.

In the simulated IR spectrum of 2A (Fig.2), the free  $\nu_{\text{OH}}$  modes appear at  $3650$  and  $3556\text{ cm}^{-1}$ . The frequency at  $3158\text{ cm}^{-1}$  corresponds to the  $\nu_{\text{CH}}$  motion. The peak at  $2813\text{ cm}^{-1}$  is attributed to the  $\text{OH}\cdots\pi$  H-bonded O–H stretching, which is remarkably blue-shifted by  $777\text{ cm}^{-1}$  with respect to that in 1A. A new type of absorption peak is observed around  $1963\text{ cm}^{-1}$  in 2A as compared to 1A, which is assigned to the  $\text{OH}\cdots\text{O}$  H-bonded O–H stretching (labeled  $\nu_{\text{OH}\cdots\text{O}}$ ). For 2B, the free  $\nu_{\text{OH}}$ ,  $\nu_{\text{CH}}$ , and  $\nu_{\text{OH}\cdots\pi}$  modes are calculated around  $3560$ ,  $3000$ , and  $1800\text{ cm}^{-1}$ , respectively.

#### 3. $n=3$

The lowest energy isomer (3A) could be regarded as the derivative of 2A, in which the third  $\text{H}_2\text{O}$  occupies the remaining free OH site of  $\text{H}_3\text{O}^+$  (Fig.1). In the

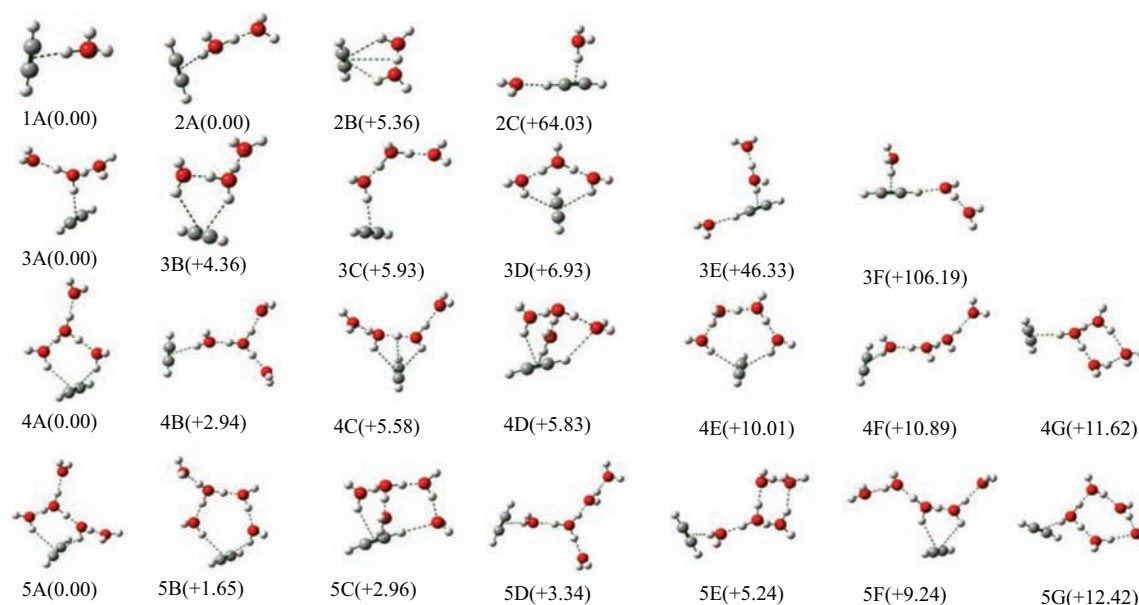


FIG. 1 Optimized structures of the  $\text{H}^+(\text{C}_2\text{H}_2)(\text{H}_2\text{O})_n$  ( $n=1-5$ ) clusters (C: gray; H: light gray; O: red). Relative energies are given in parenthesis with unit of kJ/mol.

TABLE I Scaled vibrational frequencies (in  $\text{cm}^{-1}$ ) and intensities (km/mol, in parenthesis) of free O–H stretching (free  $\nu_{\text{OH}}$ ), OH $\cdots$ O H-bonded O–H stretching ( $\nu_{\text{OH}\cdots\text{O}}$ ), OH $\cdots\pi$  H-bonded O–H stretching ( $\nu_{\text{OH}\cdots\pi}$ ), and C–H stretching of  $\text{C}_2\text{H}_2$  ( $\nu_{\text{CH}}$ ) for the lowest-lying isomers of  $\text{H}^+(\text{C}_2\text{H}_2)(\text{H}_2\text{O})_n$  ( $n=1-5$ ).

Species	Free $\nu_{\text{OH}}$	$\nu_{\text{CH}}$	$\nu_{\text{OH}\cdots\pi}$	$\nu_{\text{OH}\cdots\text{O}}$
1A	3536 (357)	3240 (1)	2036 (2659)	
	3449 (197)	3134 (243)		
2A	3650 (235)	3262 (1)	2813 (1792)	1963 (2623)
	3561 (133)	3158 (194)		
	3555 (211)			
3A	3672 (210)	3271 (0)	3078 (1398)	2537 (1680)
	3668 (171)	3168 (176)		2420 (3764)
	3578 (58)			
	3575 (82)			
4A	3684 (179)	3270 (1)	3539 (248)	2776 (901)
	3654 (194)	3166 (173)	3532 (33)	2600 (2992)
	3651 (351)			2505 (2592)
	3587 (57)			
5A	3691 (151)	3275 (1)	3583 (391)	3204 (1138)
	3688 (157)	3171 (161)	3544 (105)	2931 (1317)
	3660 (255)			2777 (2131)
	3595 (19)			2022 (3272)
	3591 (48)			

next energetically low-lying isomer 3B (+4.36 kJ/mol), one H-bonded ring is formed by two OH $\cdots\pi$  H-bonds and one OH $\cdots$ O H-bond. 3C(+5.93 kJ/mol) is evolved from 2A, in which the third water is attached by one H-bonded interaction with the second water. In 3D (+6.93 kJ/mol), two terminal water molecules in the  $\text{H}_7\text{O}_3^+$  chain form two OH $\cdots\pi$  H-bonds with  $\text{C}_2\text{H}_2$ , re-

sulting in one H-bonded three-water ring. The isomers 3E (+46.33 kJ/mol) and 3F (+106.19 kJ/mol) could be viewed as the derivative of 2C, in which the third water binds to the OH group of  $\text{H}_3\text{O}^+$  and  $\text{H}_2\text{O}$ , respectively.

In the simulated IR spectra of 3A–3F (Fig.3), the free O–H stretching vibrations weakly appear around  $3600\text{ cm}^{-1}$ . The intensities of C–H stretching vibrati-

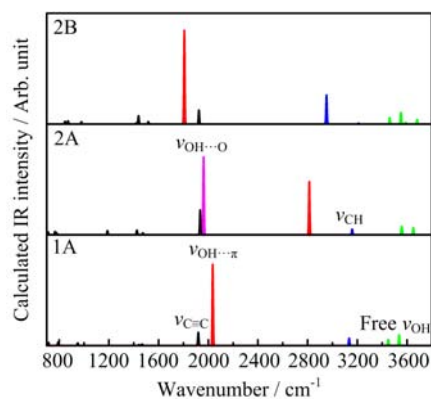


FIG. 2 Simulated IR spectra of the optimized isomers of  $\text{H}^+(\text{C}_2\text{H}_2)(\text{H}_2\text{O})_{1,2}$ . Assignments of free O–H stretching, OH $\cdots\pi$  H-bonded O–H stretching, OH $\cdots\text{O}$  H-bonded O–H stretching, and C–H stretching of  $\text{C}_2\text{H}_2$ , are indicated in green, red, magenta, and blue, respectively.

ons are very weak (around  $3200\text{ cm}^{-1}$ ) in 3A–3D, but recover remarkably in 3E and 3F because of the formation of CH $\cdots\text{O}$  H-bonds. The  $\nu_{\text{OH}\cdots\pi}$  motion presents at  $3078, 3423, 3247, 3524/3518, 2655,$  and  $1725\text{ cm}^{-1}$  in 3A–3F, respectively. The  $\nu_{\text{OH}\cdots\text{O}}$  peaks are observed around  $1800\text{--}2500\text{ cm}^{-1}$  in 3A–3E and  $3400\text{ cm}^{-1}$  in 3F.

#### 4. $n=4$ and 5

For the  $n=4$  cluster, the isomer 4A could be viewed as the derivative of 3D, in which the fourth water binds to the free OH group of the  $\text{H}_3\text{O}^+$  moiety (Fig.1). 4B is the analogy of 3C, which lies  $2.94\text{ kJ/mol}$  higher in energy above 4A. In 4C ( $+5.58\text{ kJ/mol}$ ), the fourth water is attached to the free OH group of the  $\text{H}_5\text{O}_2^+$  moiety of 3B, of which the shared proton also forms one H $\cdots\pi$  interaction with acetylene with the bond distance of  $2.97\text{ \AA}$  [30]. Analogous to 4A, 4D holds one additional CH $\cdots\text{O}$  H-bond between  $\text{H}_2\text{O}$  and  $\text{C}_2\text{H}_2$ , which lies  $+5.83\text{ kJ/mol}$  above 4A. In the structure of 4E ( $+10.01\text{ kJ/mol}$ ), one H-bonded ring is formed by two OH $\cdots\pi$  H-bonds and four H-bonds. In 4E, the distance between the shared proton and the center of  $\text{C}_2\text{H}_2$  is so long ( $4.41\text{ \AA}$ ) that there is no H $\cdots\pi$  interaction. In 4F ( $+10.89\text{ kJ/mol}$ ), one terminal of the  $\text{H}_9\text{O}_4^+$  chain forms OH $\cdots\pi$  H-bond with  $\text{C}_2\text{H}_2$ , similar to 3C. In 4G ( $+11.62\text{ kJ/mol}$ ), one ring containing four water molecules is generated and the  $\text{H}_3\text{O}^+$  moiety is incorporated into the formation of one OH $\cdots\pi$  H-bond. For the  $n=5$  cluster, the solvated structures are similar to those of  $n=4$ , suggesting that the formation of two OH $\cdots\pi$  H-bonds with the ring containing three or four water molecules is favorable.

In the simulated IR spectra of the  $n=4$  cluster (Fig.4), the  $\nu_{\text{OH}\cdots\pi}$  motion is calculated at  $3539/3532, 3355, 3584/3526, 3556/3553, 3546/3513, 3350,$  and  $3117\text{ cm}^{-1}$

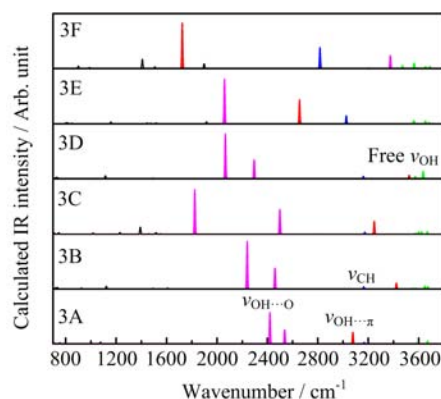


FIG. 3 Simulated IR spectra of the six optimized isomers of  $\text{H}^+(\text{C}_2\text{H}_2)(\text{H}_2\text{O})_3$ . Assignments of free O–H stretching, OH $\cdots\pi$  H-bonded O–H stretching, OH $\cdots\text{O}$  H-bonded O–H stretching, and C–H stretching of  $\text{C}_2\text{H}_2$  are indicated in green, red, magenta, and blue, respectively.

in 4A–4G, respectively. The  $\nu_{\text{OH}\cdots\text{O}}$  modes are sharply observed in all the isomers, the positions are distinctively different throughout the seven isomers. Interestingly, the characteristic vibrations of  $\text{H}_5\text{O}_2^+$  Zundel ion present around  $1600$  and  $1080\text{ cm}^{-1}$  in 4C and 4E, respectively [31].

As depicted in Fig.5, the  $\nu_{\text{OH}\cdots\pi}$  motion is predicted to be  $3583/3544, 3564/3512, 3562/3557, 3401, 3402, 3613/3516,$  and  $3223\text{ cm}^{-1}$  in 5A–5G, respectively. Several peaks of  $\nu_{\text{OH}\cdots\text{O}}$  modes remarkably appear in all the isomers. However, the vibrations of  $\text{H}_5\text{O}_2^+$  Zundel is absent from the  $n=5$  cluster.

#### B. General trend

It can be seen from the aforementioned solvation motifs that the  $\text{H}_2\text{O}$  molecules in the  $n=1\text{--}5$  clusters prefer to form the OH $\cdots\pi$  interaction rather than the CH $\cdots\text{O}$  interaction. The first solvation shell consists of one ring structure with two OH $\cdots\pi$  H-bonds and three water molecules, which is completed at  $n=4$ . Previous studies on the neutral  $(\text{C}_2\text{H}_2)(\text{H}_2\text{O})_n$  ( $n=1\text{--}4$ ) clusters revealed that the  $\text{H}_2\text{O}$  molecules prefer to form the CH $\cdots\text{O}$  and OH $\cdots\text{C}$  H-bonds with  $\text{C}_2\text{H}_2$ , and  $\text{C}_2\text{H}_2$  is involved in the formation of a H-bonded ring starting at  $n=2$ . At  $n=4$ , the neutral  $(\text{C}_2\text{H}_2)(\text{H}_2\text{O})_4$  cluster holds a water tetramer interacting with acetylene [21], which is different from the protonated  $\text{H}^+(\text{C}_2\text{H}_2)(\text{H}_2\text{O})_4$  cluster that contains a water trimer interacting with acetylene.

IR spectra of the lowest-lying isomers for the  $\text{H}^+(\text{C}_2\text{H}_2)(\text{H}_2\text{O})_n$  ( $n=1\text{--}5$ ) clusters are compared in Fig.6. It can be seen that the intensities of free O–H stretching and C–H stretching are very weak, and their positions slightly change with the increase of cluster size. The OH $\cdots\pi$  H-bonded O–H stretching is predicted at  $2036, 2813, 3078, 3532/3539,$  and  $3544/3583\text{ cm}^{-1}$

TABLE II Electron density ( $\rho(r_b)$ ), Laplacian of electron density ( $\nabla^2\rho(r_b)$ ), and energy density ( $H_{\text{BCP}}$ ) at the OH $\cdots\pi$  H-bond critical points in the lowest-lying isomers (1A–5A). Scaled vibrational frequencies of OH $\cdots\pi$  H-bonded O–H stretching ( $\nu_{\text{OH}\cdots\pi}$ ) and their red-shifts ( $\Delta\nu_{\text{OH}\cdots\pi}$ ) from the antisymmetric stretching vibrational frequency ( $3756\text{ cm}^{-1}$ ) of the free water molecule are also given.

Species	$\rho(r_b)/\text{Arb.unit}$	$\nabla^2\rho(r_b)/\text{Arb.unit}$	$H_{\text{BCP}}/\text{Arb.unit}$	$\nu_{\text{OH}\cdots\pi}/\text{cm}^{-1}$	$\Delta\nu_{\text{OH}\cdots\pi}/\text{cm}^{-1}$
1A	0.0584	0.0602	-0.0134	2036	1718
2A	0.0362	0.0759	-0.0007	2813	943
3A	0.0287	0.0715	0.0017	3078	678
4A	0.0126	0.0362	0.0012	3532	224
	0.0125	0.0362	0.0012	3539	217
5A	0.0124	0.0360	0.0012	3544	212
	0.0118	0.0338	0.0011	3583	173

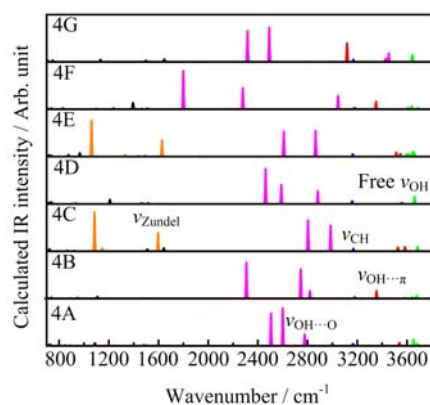


FIG. 4 Simulated IR spectra of the seven optimized isomers of  $\text{H}^+(\text{C}_2\text{H}_2)(\text{H}_2\text{O})_4$ . Assignments of free O–H stretching, OH $\cdots\pi$  H-bonded O–H stretching, OH $\cdots\text{O}$  H-bonded O–H stretching, C–H stretching of  $\text{C}_2\text{H}_2$ , and diagnostic vibration of  $\text{H}_5\text{O}_2^+$  are indicated in green, red, magenta, blue, and orange, respectively.

for 1A–5A (Table II), respectively, exhibiting an obvious increase with the increase of cluster size. This implies that the OH $\cdots\pi$  interaction strength is weakened gradually as the number of the water molecule increases, consequently, resulting in a decrease trend of the red-shift ( $\Delta\nu_{\text{OH}\cdots\pi}$ , Table II) from the antisymmetric stretching vibrational frequency ( $3756\text{ cm}^{-1}$ ) of the free water molecule [32]. Furthermore, the  $\Delta\nu_{\text{OH}\cdots\pi}$  values are very similar at  $n=4$  or 5, suggesting that the solvation of acetylene by protonated water approaches to be converged around  $n=4$  or 5. The  $\nu_{\text{OH}\cdots\text{O}}$  motions are also blue-shifted from 2A to 5A, but are split into several peaks and expanded in a broad region at larger clusters, indicating a less sensitive probe than the  $\nu_{\text{OH}\cdots\pi}$  motion for exploring early stage solvation of acetylene by adding one water molecule at a time.

Topological parameters of OH $\cdots\pi$  H-bonds at bond critical points are calculated to assess the effect of protonated water molecules on the  $\nu_{\text{OH}\cdots\pi}$  frequency shift. Electron density ( $\rho(r_b)$ ), Laplacian of electron density ( $\nabla^2\rho(r_b)$ ), and energy density ( $H_{\text{BCP}}$ ) of OH $\cdots\pi$

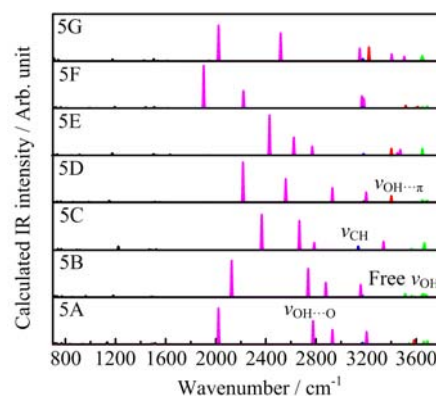


FIG. 5 Simulated IR spectra of the seven optimized isomers of  $\text{H}^+(\text{C}_2\text{H}_2)(\text{H}_2\text{O})_5$ . Assignments of free O–H stretching, OH $\cdots\pi$  H-bonded O–H stretching, OH $\cdots\text{O}$  H-bonded O–H stretching, and C–H stretching of  $\text{C}_2\text{H}_2$  are indicated in green, red, magenta, and blue, respectively.

H-bond at bond critical points (BCPs) in the lowest-lying isomers (1A–5A) are summarized in Table II. The  $\rho(r_b)$  value for 1A–5A is calculated to be 0.0584, 0.0287, 0.0362, 0.0126/0.0125, and 0.0124/0.0118 (Table II), respectively, indicating a monotonic decrease of OH $\cdots\pi$  H-bond strength. This supports the red-shifts of OH $\cdots\pi$  H-bonded O–H stretching vibrational frequencies from the free water molecule as a function of the number of water molecule (Fig.7). The negative  $H_{\text{BCP}}$  values for 1A (-0.0134) and 2A (-0.0007) suggest the OH $\cdots\pi$  H-bonds could be regarded as partially covalent interactions. The  $H_{\text{BCP}}$  values become positive in the 3A–5A clusters, indicating that the OH $\cdots\pi$  H-bonds could be mainly dominant by electrostatic interactions and thus get weaker as the cluster size increases [5].

Infrared photodissociation (IRPD) spectroscopy of mass-selected complexes has emerged as a powerful tool for the structural characterization of the gas-phase species [33–36]. Under readily achievable experimental conditions, absorption of single IR photon or multiple IR photons by a cluster can induce a measurable increase in the sequence, resulting in IRPD spectra

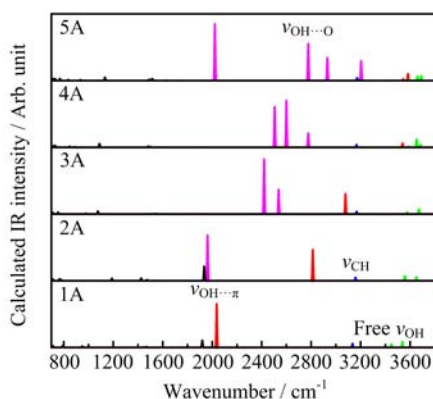


FIG. 6 Simulated IR spectra of the lowest-lying isomers of  $\text{H}^+(\text{C}_2\text{H}_2)(\text{H}_2\text{O})_n$  ( $n=1-5$ ). Assignments of free O–H stretching,  $\text{OH}\cdots\pi$  H-bonded O–H stretching,  $\text{OH}\cdots\text{O}$  H-bonded O–H stretching, and C–H stretching of  $\text{C}_2\text{H}_2$  are indicated in green, red, magenta, and blue, respectively.

that closely resemble linear absorption spectra. Compared with the conventional vibrational spectroscopy, IRPD has advantages of high selectivity, high sensitivity and being a background-free consequence technique. Considering that the free O–H stretching, H-bonded O–H stretching, and diagnostic vibration of  $\text{H}_5\text{O}_2^+$  have been successfully resolved in the IRPD spectra of a series of mass-selected clusters radiated by optical parametric oscillator/optical parametric amplifier table-top laser system or infrared free electron laser source [31, 37–39], the predicted IR spectra for the  $\text{H}^+(\text{C}_2\text{H}_2)(\text{H}_2\text{O})_n$  ( $n=1-5$ ) clusters could be readily measured by the IRPD technique and thus afford useful information for the understanding of early stage solvation of acetylene by adding one water molecule at a time.

#### IV. CONCLUSION

The solvation of acetylene by protonated water molecules has been studied via a cluster model. Quantum chemical calculations of the  $\text{H}^+(\text{C}_2\text{H}_2)(\text{H}_2\text{O})_n$  ( $n=1-5$ ) clusters indicate that the  $\text{H}_2\text{O}$  molecules prefer to form the  $\text{OH}\cdots\pi$  interaction rather than the  $\text{CH}\cdots\text{O}$  interaction. The first solvation shell consists of one ring structure with two  $\text{OH}\cdots\pi$  H-bonds and three water molecules, which is completed at  $n=4$ . Simulated IR spectra reveal that vibrational frequencies of  $\text{OH}\cdots\pi$  H-bonded O–H stretching afford a sensitive probe for exploring the solvation of acetylene by protonated water molecules. The combination of IRPD technique and theoretical modeling thus provide a vivid physical picture about how protonated water molecules solvate the acetylene.

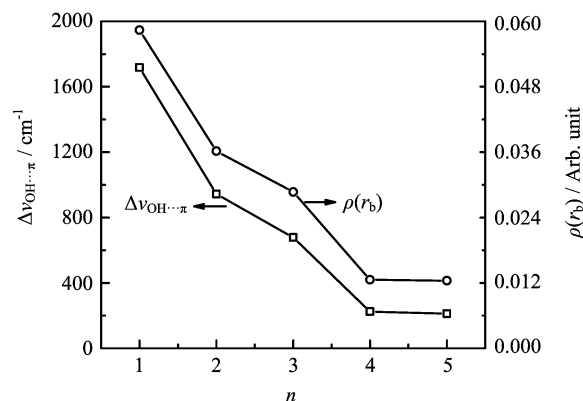


FIG. 7 Red-shifts ( $\Delta\nu_{\text{OH}\cdots\pi}$ ) of  $\text{OH}\cdots\pi$  H-bonded O–H stretching vibrational frequencies from the antisymmetric stretching vibrational frequency ( $3756 \text{ cm}^{-1}$ ) of the free water molecule and electron density ( $\rho(r_b)$ ) of the  $\text{OH}\cdots\pi$  H-bond critical points as a function of the number of water molecule ( $n$ ).

#### V. ACKNOWLEDGMENTS

This work was supported by the National Natural Science Foundation of China (No.21273232 and No.21327901) and the Key Research Program of the Chinese Academy of Science (No.KGZD-EW-T05). Ling Jiang acknowledges Hundred Talents Program of Chinese Academy of Sciences and Collaborative Innovation Center of Chemistry for Energy and Materials.

- [1] G. A. Jeffrey and W. Saenger, *Hydrogen Bonding in Biological Structures*, Berlin: Springer-Verlag (1991).
- [2] G. A. Jeffrey, *An Introduction to Hydrogen Bonding*, New York: Oxford University Press (1997).
- [3] G. R. Desiraju and T. Steiner, *The Weak Hydrogen Bond in Structural Chemistry and Biology*, New York: Oxford University Press Inc. (1999).
- [4] T. Steiner, *Angew. Chem. Int. Ed.* **41**, 48 (2002).
- [5] S. Janusz Grabowski, *Chem. Rev.* **111**, 2597 (2011).
- [6] N. Heine and K. R. Asmis, *Int. Rev. Phys. Chem.* **34**, 1 (2015).
- [7] P. A. Hunt, C. R. Ashworth, and R. P. Matthews, *Chem. Soc. Rev.* **44**, 1257 (2015).
- [8] I. Alkorta, I. Rozas, and J. Elguero, *Chem. Soc. Rev.* **27**, 163 (1998).
- [9] P. Hobza and Z. Havlas, *Chem. Rev.* **100**, 4253 (2000).
- [10] S. J. Grabowski, *J. Phys. Chem. A* **105**, 10739 (2001).
- [11] L. Sobczyk, S. J. Grabowski, and T. M. Krygowski, *Chem. Rev.* **105**, 3513 (2005).
- [12] S. Tsuzuki and A. Fujii, *Phys. Chem. Chem. Phys.* **10**, 2584 (2008).
- [13] B. G. de Oliveira, *Phys. Chem. Chem. Phys.* **15**, 37 (2013).
- [14] S. Suzuki, P. G. Green, R. E. Bumgarner, S. Dasgupta, W. A. Goddard, and G. A. Blake, *Science* **257**, 942 (1992).
- [15] R. N. Pribble and T. S. Zwier, *Science* **265**, 75 (1994).

- [16] D. A. Rodham, S. Suzuki, R. D. Suenram, F. J. Lovas, S. Dasgupta, W. A. Goddard, and G. A. Blake, *Nature* **362**, 735 (1993).
- [17] S. Tsuzuki, K. Honda, T. Uchimaru, M. Mikami, and K. Tanabe, *J. Am. Chem. Soc.* **122**, 11450 (2000).
- [18] K. Shibasaki, A. Fujii, N. Mikami and S. Tsuzuki, *J. Phys. Chem. A* **110**, 4397 (2006).
- [19] P. Tarakeshwar, H. S. Choi, and K. S. Kim, *J. Am. Chem. Soc.* **123**, 3323 (2001).
- [20] D. Tzeli, A. Mavridis, and S. S. Xantheas, *J. Chem. Phys.* **112**, 6178 (2000).
- [21] D. Tzeli, A. Mavridis, and S. S. Xantheas, *Chem. Phys. Lett.* **340**, 538 (2001).
- [22] D. Tzeli, A. Mavridis, and S. S. Xantheas, *J. Phys. Chem. A* **106**, 11327 (2002).
- [23] M. J. Frisch, G. W. Trucks, H. B. Schlegel, G. E. Scuseria, M. A. Robb, J. R. Cheeseman, G. Scalmani, V. Barone, B. Mennucci, G. A. Petersson, H. Nakatsuji, M. Caricato, X. Li, H. P. Hratchian, A. F. Izmaylov, J. Bloino, G. Zheng, J. L. Sonnenberg, M. Hada, M. Ehara, K. Toyota, R. Fukuda, J. Hasegawa, M. Ishida, T. Nakajima, Y. Honda, O. Kitao, H. Nakai, T. Vreven, J. A. Montgomery Jr., J. E. Peralta, F. Ogliaro, M. J. Bearpark, J. Heyd, E. N. Brothers, K. N. Kudin, V. N. Staroverov, R. Kobayashi, J. Normand, K. Raghavachari, A. P. Rendell, J. C. Burant, S. S. Iyengar, J. Tomasi, M. Cossi, N. Rega, N. J. Millam, M. Klene, J. E. Knox, J. B. Cross, V. Bakken, C. Adamo, J. Jaramillo, R. Gomperts, R. E. Stratmann, O. Yazyev, A. J. Austin, R. Cammi, C. Pomelli, J. W. Ochterski, R. L. Martin, K. Morokuma, V. G. Zakrzewski, G. A. Voth, P. Salvador, J. J. Dannenberg, S. Dapprich, A. D. Daniels, Ö. Farkas, J. B. Foresman, J. V. Ortiz, J. Cioslowski, and D. J. Fox, *Gaussian 09, Rev. A.02*, Wallingford CT: Gaussian, Inc., (2009).
- [24] K. L. Copeland and G. S. Tschumper, *J. Chem. Theory Comput.* **8**, 1646 (2012).
- [25] S. R. Gadre, S. D. Yeole, and N. Sahu, *Chem. Rev.* **114**, 12132 (2014).
- [26] X. B. Wang and S. R. Kass, *J. Am. Chem. Soc.* **136**, 17332 (2014).
- [27] Z. Zhao, X. T. Kong, X. Lei, B. B. Zhang, J. J. Zhao, and L. Jiang, *Chin. J. Chem. Phys.* **28**, 501 (2015).
- [28] G. E. Douberly, A. M. Ricks, B. W. Ticknor, W. C. McKee, P. v. R. Schleyer, and M. A. Duncan, *J. Phys. Chem. A* **112**, 1897 (2008).
- [29] T. Lu and F. Chen, *J. Comput. Chem.* **33**, 580 (2012).
- [30] S. J. Grabowski, *J. Phys. Chem. A* **111**, 13537 (2007).
- [31] K. R. Asmis, N. L. Pivonka, G. Santambrogio, M. Brummer, C. Kaposta, D. M. Neumark, and L. Woste, *Science* **299**, 1375 (2003).
- [32] L. Jiang, T. Wende, R. Bergmann, G. Meijer, and K. R. Asmis, *J. Am. Chem. Soc.* **132**, 7398 (2010).
- [33] E. J. Bieske and O. Dopfer, *Chem. Rev.* **100**, 3963 (2000).
- [34] M. A. Duncan, *Int. Rev. Phys. Chem.* **22**, 407 (2003).
- [35] K. R. Asmis and D. M. Neumark, *Acc. Chem. Res.* **45**, 43 (2012).
- [36] A. B. Wolk, C. M. Leavitt, E. Garand, and M. A. Johnson, *Acc. Chem. Res.* **47**, 202 (2014).
- [37] J. M. Headrick, E. G. Diken, R. S. Walters, N. I. Hammer, R. A. Christie, J. Cui, E. M. Myshakin, M. A. Duncan, M. A. Johnson, and K. D. Jordan, *Science* **308**, 1765 (2005).
- [38] A. Fujii and K. Mizuse, *Int. Rev. Phys. Chem.* **32**, 266 (2013).
- [39] J. A. Fournier, C. J. Johnson, C. T. Wolke, G. H. Weddle, A. B. Wolk, and M. A. Johnson, *Science* **344**, 1009 (2014).